Robustness control for nonlinear systems based on homogeneous prescribed sliding mode control

Do Xuan Phu[1,*], Nguyen Quoc Hung[2]

ABSTRACT

This paper presents a new homogeneous control using dual sliding mode control, and robustness control using linear matrix inequality (LMI) constraints. The controller is applied for the severe disturbance. A sliding surface function, which relates to an exponential function and itself t-norm, is applied to save the energy consumption of the control system. The constraints related LMI are proposed with the matrices and vectors of the systems following the chosen matrices in control the energy for control. Solution of the constraints is also presented with new approach to save the time of calculation. In addition, the proof for the proposed controller is also presented by using the candidate Lyapunov function. In the input control function, the t-norm type is embedded to improve its performance in control disturbance. Besides of the t-norm, the modified sliding surface in the input control is also improve the energy for controlling. The combination of these robustness control elements would bring a new view for the design of control. The advantages of the controller are demonstrated via computer simulation for a seat suspension system. A magneto-rheological fluid seat suspension with its random disturbances is used. To prove the flexibility of the controller, the proposed approach is compared with an existing controller. The compared control has the same structure as shown in the proposed model. However, its design has a disadvantage in control the severe disturbance. The comparison between two controls is a clear view of distinct improvement. The results of simulations show that the controller provides better performance and stability of the system. The stability is also analyzed through the variation of the input control and power spectral density related energy consumption.

Key words: Homogeneous control, sliding mode control, sliding surface, vibration control, seat suspension

[1]*Department of Mechatronics and Sensor Systems Technology, Vietnamese-German University, Binh Duong, Vietnam*

[2]*Department of Computational Engineering, Vietnamese-German University, Binh Duong, Vietnam*

Correspondence

Do Xuan Phu, Department of Mechatronics and Sensor Systems Technology, Vietnamese-German University, Binh Duong, Vietnam

Email: phu.dx@vgu.edu.vn

Check for updates

VNU-HCM Press

INTRODUCTION

Nowadays, the development of modern controls is continuously bringing new surprises in our life through its application such as robotic manipulators, transportations, upper and lower limb exoskeleton, etc. In this development, adaptive controller and its modification with other controls such as proportional-integral-derivative, sliding mode control, prescribed performance, etc. were presented in many featured types of research. Firstly, adaptive fuzzy control with prescribed performance was studied [1,2]. The objective of the prescribed performance [1,2] was to set up upper and lower boundaries for the error of the system. The Nussbaum function was used for unknown direction [2]. Hence the combination of both the Nussbaum function and the prescribed performance was improved the responses [2]. The model of adaptive fuzzy controller with sliding mode controller was studied [3,4]. Sliding mode control [3,4] was conventional types such as the integral model [3] and classical model [4]. However, the classical Lyapunov function was embedded in the input control function [4] to improve performance. The Lyapunov function [4] was a special case of the Riccati equation with an assumption of stability based on the removal of matrix and vector system. It is remarked that the type 1 fuzzy model was applied [1–4]. The neural networks model was also used in adaptive control [5]. The conventional PID model was applied [5] for the design of adaptation laws. This PID model was also used [6–8]. It was a similar structure in control [5,6], especially in adaptation laws. PID was applied in design the PID-like sliding surface of sliding model control [7]. It is noteworthy that PID could be used in two types: adaptation laws [5,6,8], sliding surface [8]. The adaptive fuzzy control was also presented [9–11]. The interval type 2 fuzzy model was applied [8–11]. This point is different from the others [1–4,6,7]. The Riccati-like equation was adopted [8–11], and this utilization was different from the properties of the system: disturbance, vibration control, consumption of energy. The sliding mode control was utilized as a first step to combine controls in adaptation laws. Besides, optimal control was also used in the design of adaptive control [10]. The

application of sliding mode control was shown [12–18]. In these applications, the conventional sliding surface was used. Detail models of sliding surface are analyzed as follows. The saturation function of sliding mode control was applied [12]. The sliding surface [12] was obtained by using a PID-like model, and the saturation function was used in the input control. The signum function was also used in input control [13–15,17,18]. It is noteworthy that there are two types of function related to the conventional input control of sliding mode control: saturation function and signum function. The disadvantage of these functions is the chattering phenomenon and sensitive to disturbances. However, these functions could be improved by combining with forms of sliding surface as terminal type (or twisting type) [13,15], classical type [14,18], and integral type [16].

From the above analysis, the adaptive control has remained as a potential controller for modern devices. It can be defined with other control types such as sliding mode control [3,4,7–12,17], optimal control [10], prescribed performance [1,2,9], Riccati-like equation [4,8–11], fuzzy model [1–4,7–11], and neural networks [6] for improving the performance of the system. However, the model of sliding mode control [3,4,7–12,17,18] is conventional and this can remain a disadvantage when applying for control design. Hence, in this research, a new novel form of homogeneous controller, which preserves the merits of sliding mode control based on prescribed performance and linear matrix inequality, will be developed. The proposed control is to follow the objective as a simple model and its advantage in control severe disturbance. The main contributions are summarized as follows:

(1) A new integration of classical sliding surface, prescribed form of sliding surface and linear matrix inequality for homogeneous control is presented.

(2) A new proof for the design of a homogeneous controller with a new sliding surface of sliding mode control is proposed.

(3) The outstanding property of the proposed approach is validated in simulation for a seat suspension system and compared with a controller [19].

The rest of this article is organized as follows. In section 2, the proposed design is presented. In section 3, the simulation for two controls including the proposed control, the compared control [19] is described. Finally, the conclusion is presented in section 4 with the main results of the above sections.

DESIGN METHOD OF A HOMOGENEOUS PRESCRIBED SLIDING MODE CONTROL

The control is developed based on a SISO (single-input single-output) nonlinear system as follows:

$$\dot{x}_\nabla = f_\nabla(x_\nabla) + g_\nabla(x_\nabla)u_\nabla(t) + d_\nabla(t) \tag{1}$$

Where $f_\nabla(x_\nabla) \in R^n$ and $g_\nabla(x_\nabla) \in R^n$ are two nonlinear functions, $u_\nabla(t) \in R^1$ is input control, $d_\nabla(t) \in R^n$ is a disturbance, $|d_\nabla(t)| \le \delta t$, where the value $\delta d \in R^n$ is a bound of $d_\nabla(t)$, $x_\nabla = [x_{1\nabla}, x_{2\nabla}, ..., x_{n\nabla}] = [x_{1\nabla}, x_{1\nabla}^1, ..., x_{1\nabla}^{(n-1)}]^T \in R^n$ is state system.
A new suggestion vector is $\overrightarrow{x}_\nabla$ with its elements $\overrightarrow{x}_\nabla = \left[x_{1\nabla}, x_{2\nabla}, ...x_{(n-1)\nabla}\right]^T$. The governing system (1) can be defined as follows:

$$\overrightarrow{x}_{;v} = S_{1\nabla}x_\nabla + S_{2\nabla}^T s_{s\nabla} \tag{2}$$

where,

$$S_{1\nabla} = \begin{bmatrix} 0 & 1 & 0 & ... & 0 \\ 0 & 0 & 1 & ... & 0 \\ . & . & . & ... & . \\ -k_1 & -k_2 & -k_3 & ... & -k_{n-1} \end{bmatrix},$$

$$S_{2\nabla} = \begin{bmatrix} 0 \\ 0 \\ . \\ 1 \end{bmatrix}$$

The tracking function is described as $e_\nabla(t) = x_{1\nabla} - x_{d\nabla}$, where $x_{d\nabla}$ is the desired result related the system; k_i is Hurwitz parameters which relate to the conventional sliding mode control. It is noteworthy that $x_{1\nabla}$ is the similar value as x_∇ in Eq. (2). The prescribed sliding surface is expressed as follows [10]:

$$\sigma_{s\nabla} = \dot{\psi} + c_{s\nabla}\varphi \tag{3}$$

Where, $c_{s\nabla} > 0$ is a positive constant. The function φ is defined as follows:

$$\varphi = \frac{1}{2}\left[\ln\left(\lambda + e_\nabla(t)\right) - \ln\left(\lambda - e_\nabla(t)\right)\right] \tag{4}$$

Where $-\lambda(t) < e_\nabla(t) < \lambda(t)$, and $\lambda(t) = (\lambda(0) - \lambda(\infty))e^{-lt} + \lambda(\infty)$, $l > 0$, $\lambda(t)$ is the prescribed function.
Remark 1. *The prescribed sliding surface (3) is used to control the chattering phenomenon and then guarantee the response following desired boundaries. This advanced property is useful for the system under severe disturbance. The progress to derive the sliding surface (3) was presented [10].*
The governing system (1) can be described as follows:

$$\dot{x}_\nabla = f_\nabla(x_\nabla) + g_\nabla(x_\nabla)u_\nabla(t) + d_\nabla(t)$$
$$= A_P(x_\nabla(t), t)x_\nabla(t) + B_P(x_\nabla t, t)u_\nabla(t) + C_p D_\nabla(t) \tag{5}$$

Where, $A_P \in R^{n \times n}$, $B_P \in R^{n \times m}$, $u_\nabla \in R^m$, $C_P \in R^{n \times m}$, $D_\nabla \in R^m$ and $C_p D_\nabla(t) \leq D_s$. It is remarked that D_s is the maximal boundary of the disturbance; C_p, D_∇ are the matrix and the vector when deriving the governing equation following state-space form.

Remark 2. *Equation (5) is also a change of the property of the governing equation (1) from a nonlinear model to a linear model for the steps of the proposed controller. The linearization can be used in this step to find the linear model which belongs to the property of the system.*

The new main input u_∇ is proposed as follows:

$$u_\nabla = \alpha K_0 I_n \sigma_{s\nabla}^2 + \alpha |\sigma_{s\nabla}|^{\nu+\varepsilon} K_\zeta I_n e^{G_\zeta(-\ln||\sigma_{s\nabla}||)} \sigma_{s\nabla} \tag{6}$$

Where, $K_0 = Z_0 (\gamma W - I_n)^{-1} \in R^{m \times n}$ is a matrix $Z_0 \in R^{m \times n}$ is a Lyapunov matrix; $W \in R^{n \times n}$ is a matrix related the Lyapunov function; $\gamma \in R$, $\alpha \in R^+$ are positive constants; $K_\zeta \in R^{m \times n}$ is a matrix as $K_\zeta = ZP$; the matrices $Z \in R^{m \times n}$ and $P \in R^{n \times n}$ are chosen from the constraints; $G_\zeta \in R^{n \times n}$ is calculated as $G_\zeta = \nu W + \varepsilon I_n$, I_n is the unit matrix; $\nu \in R$, $\varepsilon \in R$ are two constants. The element of Z_0, W, K_0 and K_ζ are solved from the constraints of linear matrix inequality (LMI in short) method as Figure 1:

Remark 3. *The input (6) is a new design with the assumption that the disturbance is approximately zero. The existence of the disturbance through equation (7) with the relations of K_0, Z_0 and K_ζ will guarantee the stability of the system.*

Remark 4. *The constraint equation (7) is to follow the LMI method. In LMI, the diagonal elements are always designed less than or equal to zero. The other elements are going to zero value when analyzing to infinity of time.*

From Eq. (7), the constraints for the input control term u are derived as:

$$A_p W - W A_P^T - A_P + B_P Z_0 = 0 \tag{8}$$

$$(\gamma W - I_n) B_P < 0 \tag{9}$$

$$(A_P + B_P K_0) X + X (A_P + B_P K_0)^T + B_P Z + Z^T B_P^T + \delta_x X + D_s \leq 0 \tag{10}$$

Where, $X \in R^{n \times n}$ is chosen matrix; $\delta_x \in R$ is a positive chosen constant.

Remark 5. *The constraints (8-10) are chosen from the property of Eq. (7) based on the boundary zero. The constraints are solved by the trial-and-error method.*

Remark 6. *The parameter $\alpha \in R^+$ in Eq.(7) is chosen from the performance output control. It is remarked that the output control relates the prescribed sliding surface, the results of constraints (8-10).*

Proof of Eq.(7).

The equation (7) implies that $(-\gamma W + I_n) B_P > 0$. A proposed smooth function $\varphi(\delta_d)$ is defined as follows:

$$\varphi(\delta_d) = z^T[(A_P + B_P K_0 \delta_d) X + X(A_P + B_P K_0 \delta_d)^T + B_P Z + Z^T B_P^T + \delta_x X + D_s]z \tag{11}$$

Where, $z \in R^n, z \neq \{0\}$, z is a system variable related to the control progress. The boundary δ_d can be seen as a variable of the system, $\delta_d \in [\delta_{dmin}, 1]$. The smooth function (11) is used to depict the operation of a system with the feedback signal, disturbance, and other elements related robust system. A derivative of equation (11) is obtained as:

$$\varphi'(\delta_d) = z^T \left(B_P K_0 X + X B_P^T K_0^T \right) z \leq \frac{1}{\delta_d} z^T \left(B_P K_0 X + X B_P^T K_0^T \right) z \tag{12}$$

From the boundary of $\delta_d \in [\delta_{dmin}, 1]$, it can be determined δ_{max} as $0 < \delta_{min} \leq \delta_{max} \leq 1$. On the other hand, equation (11) can be described as Figure 2:

From the boundary of $0 < \delta_{min} \leq \delta_{max} \leq 1$, values of $\ln \frac{\delta_{dmax}}{\delta_{dmin}}$ and δ_{dmax} go to 0 and 1, respectively. Hence equation (14) is rewritten as follows as Figure 3:

Theorem: *The proposed control is designed with the input control u as shown in Eq. (6) and its constraints for improving the global stability of the system as shown in Eqs. (8-10). These functions are the frame of the controllers which is proposed for the nonlinear system following the homogeneous sliding mode control.*

Proof: The Lyapunov candidate for the proposed control is described as follows:

$$V = \frac{1}{2} \sigma_{s\nabla}^2 \tag{16}$$

Derivative form of Eq.(16) is described as:

$$\widehat{V} = \sigma_{s\nabla} \widehat{\sigma}_{s\nabla} \tag{17}$$

Eq. (5) can be defined as derivative form as:

$$\widehat{\sigma}_{s\nabla} = \dot{\widehat{\varphi}} + c_{s\nabla} \widehat{\varphi} = M_{1\nabla} + M_{2\nabla} + M_{3\nabla} \left(\widehat{\dot{x}}_\nabla - \dot{x}_{d\nabla} \right) + c_{s\nabla} \widehat{\varphi} \tag{18}$$

Where,

$$\widehat{\varphi} = \frac{1}{2} \left[\frac{\widehat{\lambda} + \widehat{e}_\nabla(t)}{\lambda + e_\nabla(t)} - \frac{\widehat{\lambda} - \widehat{e}_\nabla(t)}{\lambda - e_\nabla(t)} \right],$$

$$\dot{\widehat{\varphi}} = M_{1\nabla} + M_{2\nabla} + M_{3\nabla} \dot{\widehat{e}}_\nabla(t),$$

$$M_{1\nabla} = \frac{\dot{\widehat{\lambda}}(\lambda + e_\nabla(t)) - \left(\widehat{\lambda} + \widehat{e}_\nabla(t) \right)^2}{2(\lambda + e_\nabla(t))^2},$$

$$\left[\begin{array}{ccc} \left(A_P W - W A_P^T - A_P + B_P Z_0\right) & \sqrt{ln\frac{\delta_{dmax}}{\delta_{dmin}}} B_P Z_0 & Z_0 \, ln\frac{\delta_{dmax}}{\delta_{dmin}} \\ \sqrt{ln\frac{\delta_{dmax}}{\delta_{dmin}}} B_P^T Z_0^T & \left(\gamma W - I_n\right) B_P & 0 \\ Z_0 \, ln\frac{\delta_{dmax}}{\delta_{dmin}} & 0 & \left[\begin{array}{c} \left(A_P + B_P K_0\right) X + X \left(A_P + B_P K_0\right)^T + \\ B_P Z + Z^T B_P^T + \delta_x X + D_s \end{array} \right] \end{array} \right] \leq 0$$

$$\Leftrightarrow \left(\begin{array}{c} A_P W - W A_P^T - \\ - A_P + B_P Z_0 \end{array} \right) \left(\gamma W - I_n\right) B_P \left[\begin{array}{c} \left(A_P + B_P K_0\right) X + X \left(A_P + B_P K_0\right)^T + \\ + B_P Z + Z^T B_P^T + \delta_x X + D_s \end{array} \right] -$$

$$- Z_0^2 \, ln^2 \frac{\delta_{dmax}}{\delta_{dmin}} \left(\gamma W - I_n\right) B_P - ln\frac{\delta_{dmax}}{\delta_{dmin}} \left[\begin{array}{c} \left(A_P + B_P K_0\right) X + X \left(A_P + B_P K_0\right)^T + \\ + B_P Z + Z^T B_P^T + \delta_x X + D_s \end{array} \right] \leq 0 \tag{7}$$

Where, $\delta_{dmin}, \delta_{dmax}$ are positive parameters related the disturbance $\mathbf{D}_s$ and $\delta_{dmin} \leq \delta_{dmax}$.

Figure 1: Equation 7

$$\varphi\left(\delta_d\right) = \varphi\left(\delta_{dmax}\right) - \int_{\delta_{dmin}}^{\delta_{dmax}} \varphi'(s) ds \leq z^T \left[\begin{array}{c} \left(A_P + B_P K_0 \delta_{dmax}\right) X + X \left(A_P + B_P K_0 \delta_{dmax}\right)^T + \\ + B_P Z + Z^T B_P^T + \delta_x X + D_s \end{array} \right] z -$$

$$- ln\frac{\delta_{dmax}}{\delta_{dmin}} z^T \left(B_P K_0 X + X B_P^T K_0^T\right) z \tag{13}$$

The maximal value in Eq. (13) can be obtained as follows:

$$\varphi\left(\delta_d\right) \leq z^T \left(\begin{array}{c} A_P W - W A_P^T - \\ - A_P + B_P \left(\gamma W - I_n\right) K_0 \end{array} \right) \left(\left(\gamma W - I_n\right) B_P \right) \left(\begin{array}{c} \left(A_P + B_P K_0 \delta_{dmax}\right) X + X \left(A_P + B_P K_0 \delta_{dmax}\right)^T + \\ + B_P Z + Z^T B_P^T + \delta_x X + D_s \end{array} \right) z -$$

$$- ln\frac{\delta_{dmax}}{\delta_{dmin}} z^T \left(B_P K_0 X + X B_P^T K_0^T\right) z - z^T \left(\left(\gamma W - I_n\right)^2 K_0^2 \, ln^2 \frac{\delta_{dmax}}{\delta_{dmin}} \left(\gamma W - I_n\right) B_P \right) z -$$

$$- ln\frac{\delta_{dmax}}{\delta_{dmin}} z^T \left(\begin{array}{c} \left(A_P + B_P K_0 \delta_{dmax}\right) X + X \left(A_P + B_P K_0 \delta_{dmax}\right)^T + \\ + B_P Z + Z^T B_P^T + \delta_x X + D_s \end{array} \right) z$$

$$\tag{14}$$

Figure 2: Equation (13) and (14)

$$\varphi(\delta_d) \leq \mathbf{z}^T \begin{pmatrix} A_P W - W A_P^T - \\ -A_P + B_P(\gamma W - I_n) K_0 \end{pmatrix} ((\gamma W - I_n) B_P) \begin{pmatrix} (A_P + B_P K_0) X + X(A_P + B_P K_0)^T + \\ + B_P Z + Z^T B_P^T + \delta_x X + D_s \end{pmatrix} \mathbf{z} < 0$$

$$(15)$$

The result (15) is less than zero because $(\gamma W - I_n) B_P < 0$, $\begin{pmatrix} A_P W - W A_P^T - \\ -A_P + B_P(\gamma W - I_n) K_0 \end{pmatrix} \leq 0$, and

$\begin{pmatrix} (A_P + B_P K_0) X + X(A_P + B_P K_0)^T + \\ + B_P Z + Z^T B_P^T + \delta_x X + D_s \end{pmatrix} \leq 0$. Applying Schur's complement with $\mathbf{z}^T \mathbf{z}$ to Eq. (14), the

obtained result is Eq.(7). The proof is completed. ■

Figure 3: Equation (15)

$$M_{2\nabla} = \frac{\dot{\hat{\lambda}}(\lambda - e_\nabla(t)) - (\hat{\lambda} - \hat{e}_\nabla(t))^2}{2(\lambda - e_\nabla(t))^2},$$

$$M_{3\nabla} = \left(\frac{\lambda + e_\nabla(t)}{2(\lambda + e_\nabla(t))^2} + \frac{\lambda - e_\nabla(t)}{2(\lambda - e_\nabla(t))^2} \right).$$

Substituting Eq. (5) into Eq. (18), equation (18) is rewritten as:

$$\hat{\sigma}_{s\nabla} = \dot{\hat{\varphi}} + c_{s\nabla}\hat{\varphi} = M_{1\nabla} + M_{2\nabla} + M_{3\nabla}\left(A_P x_\nabla + B_P u_\nabla + C_P D_\nabla - \dot{\hat{x}}_{d\nabla}\right) + c_{s\nabla}\hat{\varphi} \quad (19)$$

The lumped uncertainty is then determined by

$$\psi = M_{3\nabla} C_P D_\nabla \quad (20)$$

Using Eq. (6) and Eq. (20), equation (19) is expressed as:

$$\hat{\sigma}_{s\nabla} = M_{1\nabla} + M_{2\nabla} + M_{3\nabla}A_P x_\nabla \\ + M_{3\nabla}B_P u_\nabla - M_{3\nabla}\dot{\hat{x}}_{d\nabla} + c_{s\nabla}\hat{\varphi} \\ \Leftrightarrow \hat{\sigma}_{s\nabla} = M_{1\nabla} + M_{2\nabla} + M_{3\nabla}A_P x_\nabla + M_{3\nabla}B_P \times \\ (\alpha K_0 I_n \sigma_{s\nabla}^2 + \alpha |\sigma_{s\nabla}|^{\nu+\varepsilon} K_\zeta I_n e^{G_\zeta(-\ln||\sigma_{s\nabla}||)}\sigma_{s\nabla}) \\ - M_{3\nabla}\dot{\hat{x}}_{d\nabla} + c_{s\nabla}\hat{\varphi} \quad (21)$$

Substituting Eq. (21) into Eq. (17), equation (17) is rewritten as follows:

$$\hat{V} = (M_{1\nabla} + M_{2\nabla})\sigma_{s\nabla} + M_{3\nabla}A_P x_\nabla \sigma_{s\nabla} \\ + \alpha M_{3\nabla}B_P K_0 I_n \sigma_{n\nabla}^3 + \sigma_{s\nabla}\psi + \\ \alpha M_{3\nabla}||\sigma_{s\nabla}||^{\nu+\varepsilon}B_P K_\zeta I_n e^{G_\zeta(-\ln||\sigma_{s\nabla}||)}\sigma_{s\nabla}^2 \\ - M_{3\nabla}x_{d\nabla}\sigma_{s\nabla} + c_{s\nabla}\varphi\sigma_{s\nabla} \\ \leq M_{3\nabla}A_P x_\nabla \sigma_{s\nabla} + \sigma_{s\nabla}\psi + \\ \alpha M_{3\nabla}||\sigma_{s\nabla}||^{\nu+\varepsilon}B_P K_\zeta I_n e^{G_\zeta(-\ln||\sigma_{s\nabla}||)}\sigma_{s\nabla}^2 \quad (22)$$

The boundary of Eq. (22) can be found as:

$$\hat{V} = (M_{1\nabla} + M_{2\nabla})\sigma_{s\nabla} + M_{3\nabla}A_P x_\nabla \sigma_{s\nabla} \\ + \alpha M_{3\nabla}B_P K_0 I_n \sigma_{n\nabla}^3 + \sigma_{s\nabla}\psi + \\ \alpha M_{3\nabla}||\sigma_{s\nabla}||^{\nu+\varepsilon}B_P K_\zeta I_n e^{G_\zeta(-\ln||\sigma_{s\nabla}||)}\sigma_{s\nabla}^2 \\ - M_{3\nabla}x_{d\nabla}\sigma_{s\nabla} + c_{s\nabla}\varphi\sigma_{s\nabla} \\ \leq M_{3\nabla}A_P x_\nabla \sigma_{s\nabla} + \sigma_{s\nabla}\psi + \\ \alpha M_{3\nabla}||\sigma_{s\nabla}||^{\nu+\varepsilon}B_P K_\zeta I_n e^{G_\zeta(-\ln||\sigma_{s\nabla}||)}\sigma_{s\nabla}^2 \quad (23)$$

Where, $\psi = \alpha M_{3\nabla}||\sigma_{s\nabla}||^{\nu+\varepsilon}B_P K_\zeta I_n e^{G_\zeta(-\ln||\sigma_{s\nabla}||)}$. Integrating Eq. (23) from $t = 0$ to $t = T$ is obtained as follows;

$$V(0) - V(T) + M_{3\nabla}\int_0^T A_P x_\nabla \sigma_{s\nabla}dt \\ \geq \frac{1}{2}\int_0^T \frac{\omega^2}{\sqrt{\psi}}dt \quad (24)$$

Where $V(0) = \frac{1}{2}\sigma_{s\nabla}^2(0)$. It is noteworthy that $V(T)$ is positive. So Eq. (24) is rewritten as:

$$V(0) + M_{3\nabla}\int_0^T A_P x_\nabla \sigma_{s\nabla}dt \\ \geq \frac{1}{2}\int_0^T \frac{\omega^2}{\sqrt{\psi}}dt \geq 0 \quad (25)$$

Hence the system is stable. This ends the proof. □
From the above analysis, the flow chart of the control is summarized in Figure 4. The observer[20] is used to evaluate the responses.

SIMULATION RESULTS AND DISCUSSIONS

Dynamic Seat Suspension Model

In this work, the model of vehicle suspension system[11] is used for simulation as shown in Figure 5. The main dynamic equations are described as follows.

$$m_s\dot{\hat{x}}_s = -k_s(x_s - x_0) - c_s(\hat{x}_s - \hat{x}_0) \\ + k_1(x_1 - x_s) + c_1(\hat{x}_1 - \hat{x}_s) + F_{MR} \quad (26)$$
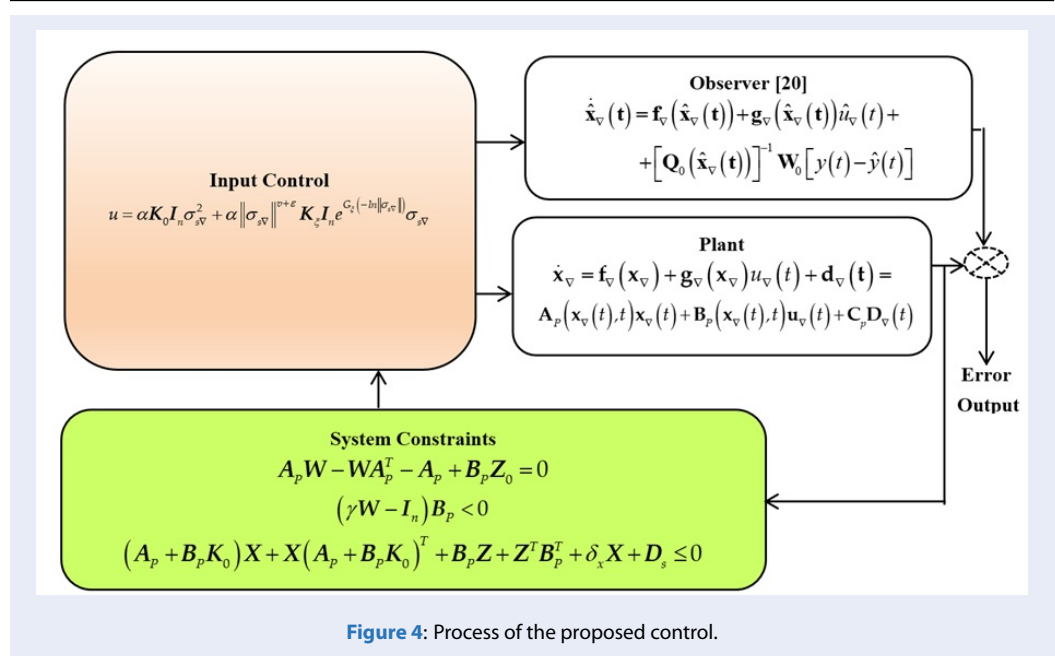
Figure 4: Process of the proposed control.

$$m_1 \dot{\hat{x}} = -k_1 (x_1 - x_s) + c_1 (\hat{x}_1 - \hat{x}_s) \tag{27}$$

Eqs.(26,27) can be rewritten as follows:

$$
\begin{aligned}
\hat{x}_{11} &= \hat{x}_s = x_{22} \\
\hat{x}_{22} &= f_{11}(x_{11}, x_{22}, x_{33}, x_{44}) \\
&\quad + g_{11}(x_{11}, x_{22}, x_{33}, x_{44}) u_\nabla \\
\hat{x}_{33} &= \hat{x}_1 = x_{44} \\
\hat{x}_{44} &= f_{22}(x_{11}, x_{22}, x_{33}, x_{44})
\end{aligned}
\tag{28}
$$

Where

$$
\begin{aligned}
f_{11}(x_{11}, x_{22}, x_{33}, x_{44}) &= \\
-\tfrac{k_s}{m_s}(x_{11} - x_0) &- \tfrac{c_s}{m_s}(x_{22} - \hat{x}_0) \\
+\tfrac{k_1}{m_s}(x_{33} - x_{11}) &+ \tfrac{c_1}{m_s}(x_{44} - x_{22}), \\
g_{11}(x_{11}, x_{22}, x_{33}, x_{44}) &= \tfrac{1}{m_s}, \\
u_\nabla &= F_{MR}, \\
f_{22}(x_{11}, x_{22}, x_{33}, x_{44}) & \\
= -\tfrac{k_1}{m_s}(x_{33} - x_{11}) &- \tfrac{c_1}{m_s}(x_{44} - x_{22}).
\end{aligned}
$$

The voltage to be applied to the damper is calculated as follows[11]:

$$
V = \frac{F_{MR} - [c_a (x_{44} - x_{22}) + k_0 (x_{33} - x_{11}) + \alpha_a \phi]}{c_b (x_{44} - x_{22}) + \alpha_b \phi} \tag{29}
$$

Two controllers are used for simulation: an existing control[19], and the proposed controller. The control[19] is also a start-of-art controller for comparison properties of the proposed control in this study. The detail parameters for the two controllers are shown in Tables 1 and 2. The random step wave road is used for simulation as excitation as shown in Figure 6. This signal is a real signal under the raw surface road which was used[9–11]. The main input control is calculated for the force damper with its bounded value is 1000 N. An observer[20] is chosen for two controls. Based on the selected parameters and the matrices, the simulation is executed and the results are shown and discussed.

DISCUSSIONS

The main results of the simulation are shown in Figure 7-Figure 15. Results of the proposed control are shown in Figure 7-Figure 11. In Figure 7, the performance of the proposed controller is good, and the initial excitation as shown in Figure 6 is decreased its values after controlling as shown in Figure 7a. Because of good performance at seat position, the vibration of the driver also decreases as shown in Figure 8. It is noteworthy that the performance of the driver is closed-relation with the seat system. Hence, any variations of the system are also directly affect the comfortable state of the driver. In Figure 9, the values of the displacement seat's response always belong to the boundary of the prescribed performance. So the obtained responses of the proposed control is to guarantee the stability of the system. In the proposed control, the prescribed sliding surface is used and its response is shown in Figure 10. In this figure, the sliding surface has changed its value following the excitation and then adjust the input control to optimize the performance. The damping force of the MR damper when using the proposed control is shown in Figure 11. It
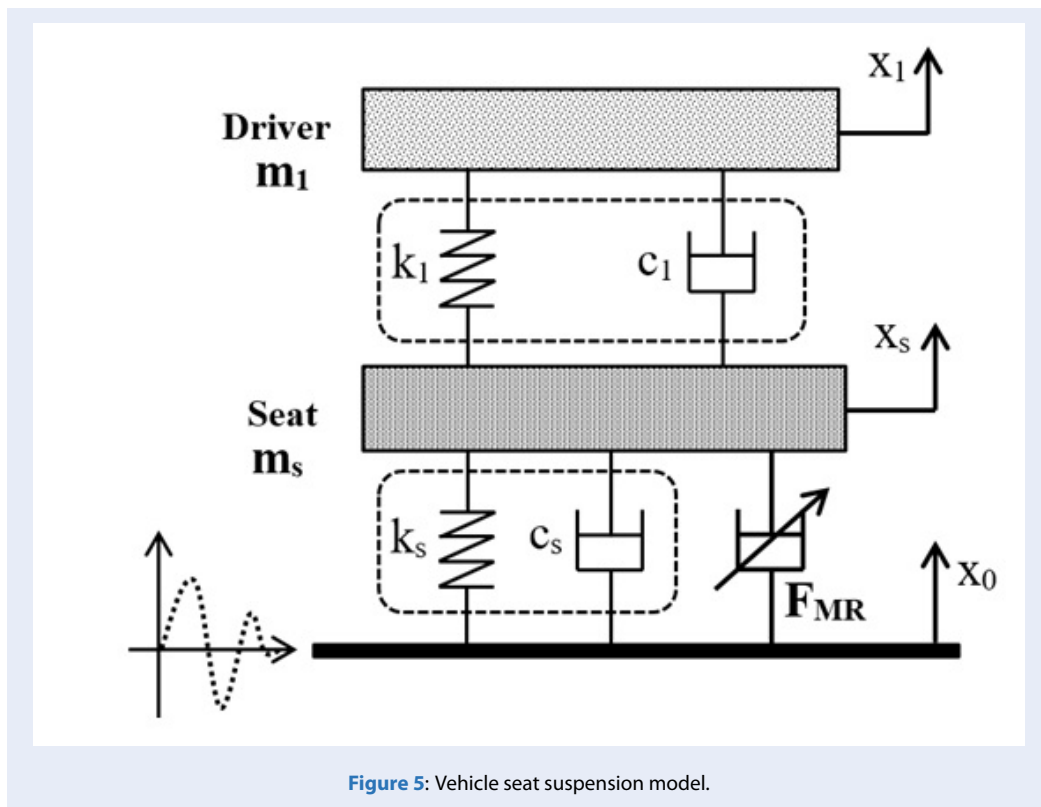
Figure 5: Vehicle seat suspension model.

Table 1: Simulation parameters for the proposed controller.

Parameter	Value
Initial value $\lambda(0)$	0.5
Infinity value λ_∞	0.001
Exponential value l	0.00047
Boundary force	1000 N
Sliding surface constants $[k_1, k_2]$	$[1, 50]$
Constant $c_{s\nabla}$	5000
Observer matrix Q_0	$[1\ \ 0; 0\ \ 1]$
Observer matrix W_0	$[30; 10]$
Initial state	$[0.035\ \ 2.5]$
Initial state for observer	$[0.035\ \ 2.5]$
Parameter γ	0.00001
Parameter α	1e-10
Parameter ν	1
Parameter ε	1
Parameter δ_x	0.5
Boundary disturbance D_s	$[3\ \ 3; 3\ \ 3]$
Chosen matrix W	$[1\ \ 1; 1\ \ 1]$

Table 2: Parameters of seat suspension system for compared control[19]. (*The symbols in this table are similar the original form[19])

Parameter	Value
Maximum damping force	1000 N
Observer matrix Q_0	$[1\ 0; 0\ 1]$
Observer matrix W_0	$[30; 10]$
Parameter γ	0.00001
Parameter ν	1
Parameter ε	1
Parameter δ	0.1
Vector y_0	$\left[-67170\quad -3.975.10^3\right]$
Matrix L	$\left[5.10^{-8}\ \ 6.10^{-10}; 5.10^{-5}\ \ 1.10^{-6}\right]$
Matrix G_d	$[1\ 1; 1\ 1]$
Initial state for control	$[0.035\ \ 2.5]$
Initial state for observer	$[0.035\ \ 2.5]$
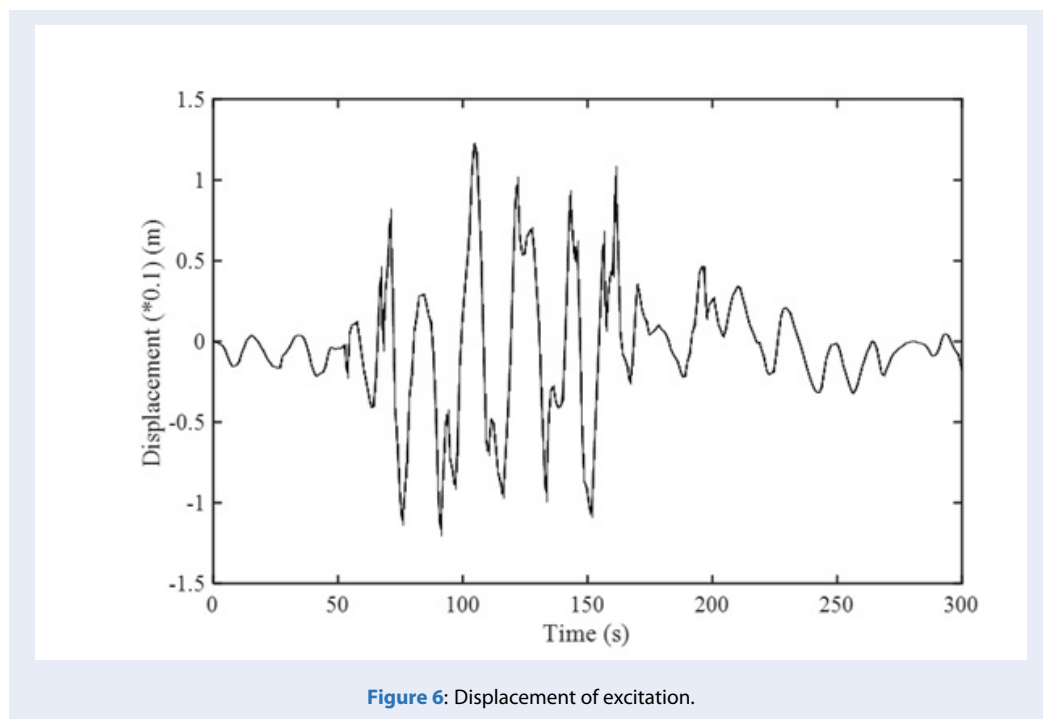
Figure 6: Displacement of excitation.
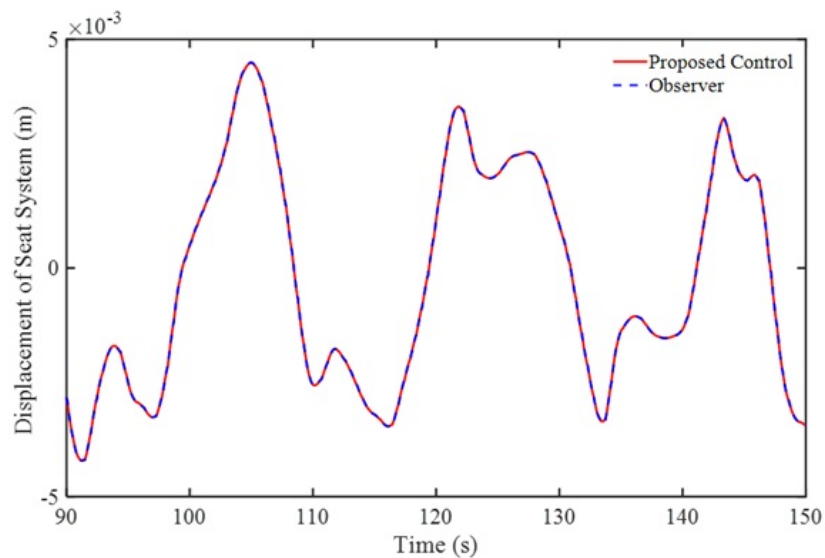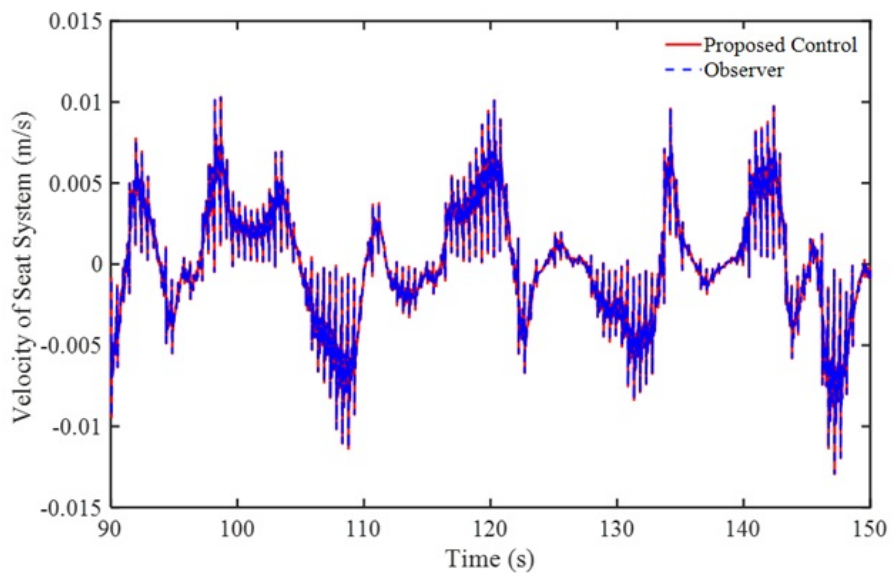
Figure 7: Displacement of seat system of the proposed control: (a) Displacement, (b) Velocity.
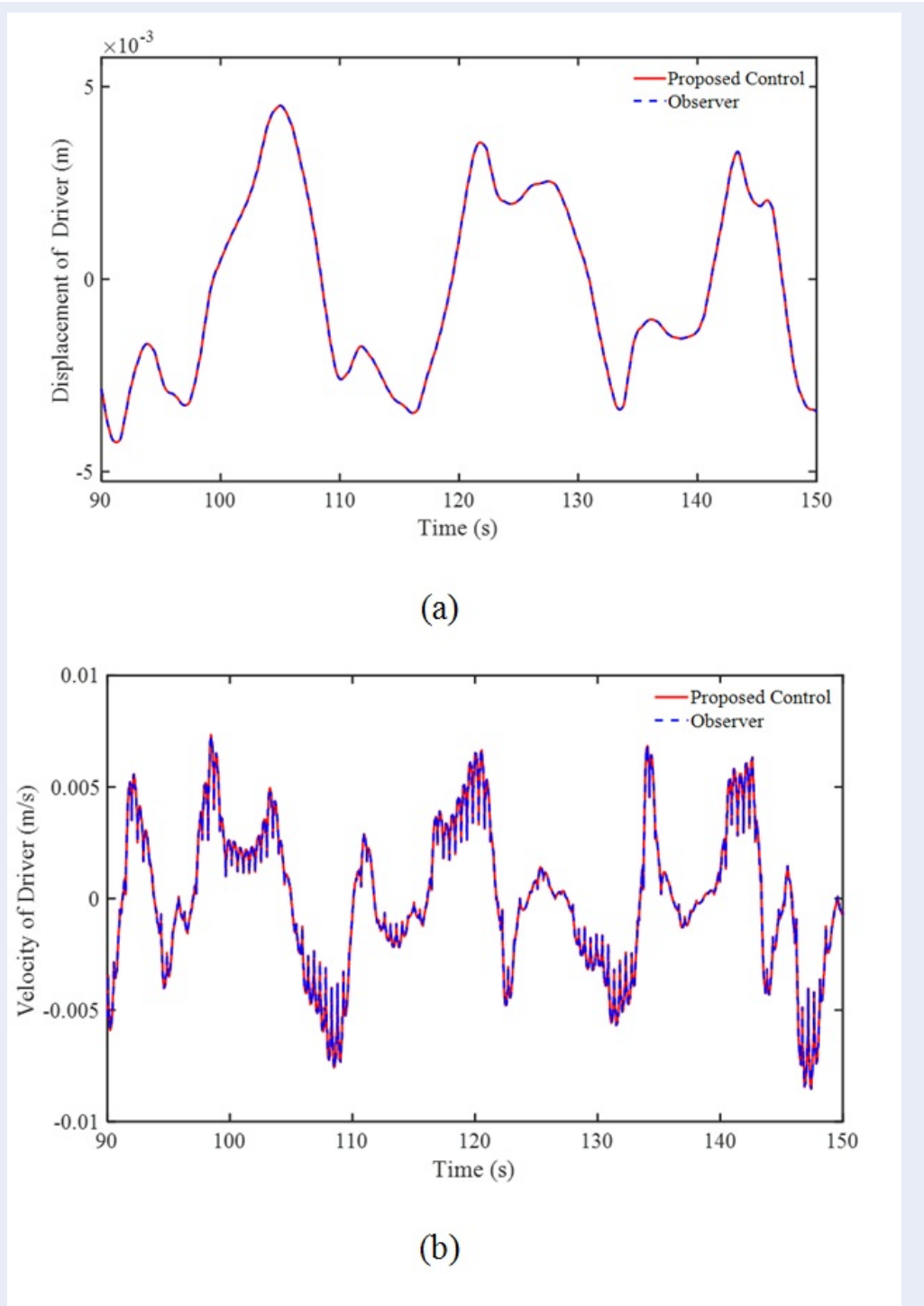
Figure 8: Displacement of driver of the proposed control: (a) Displacement, (b) Velocity.
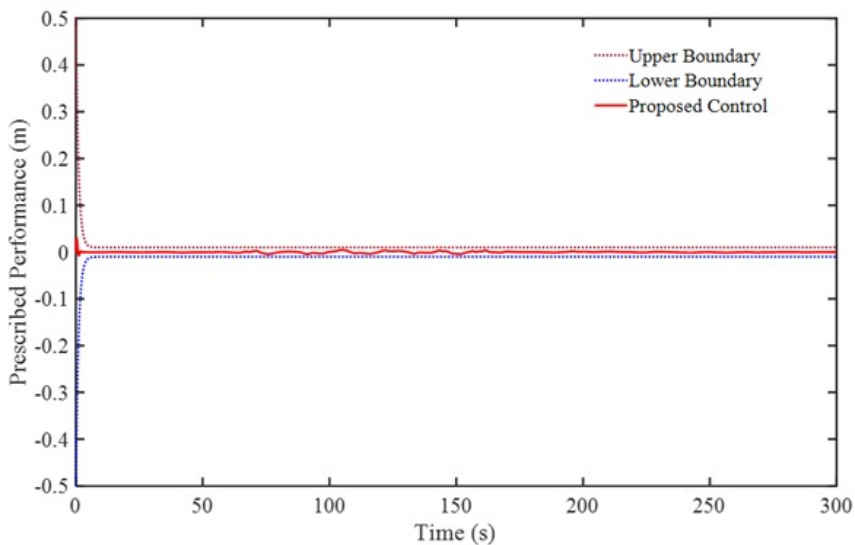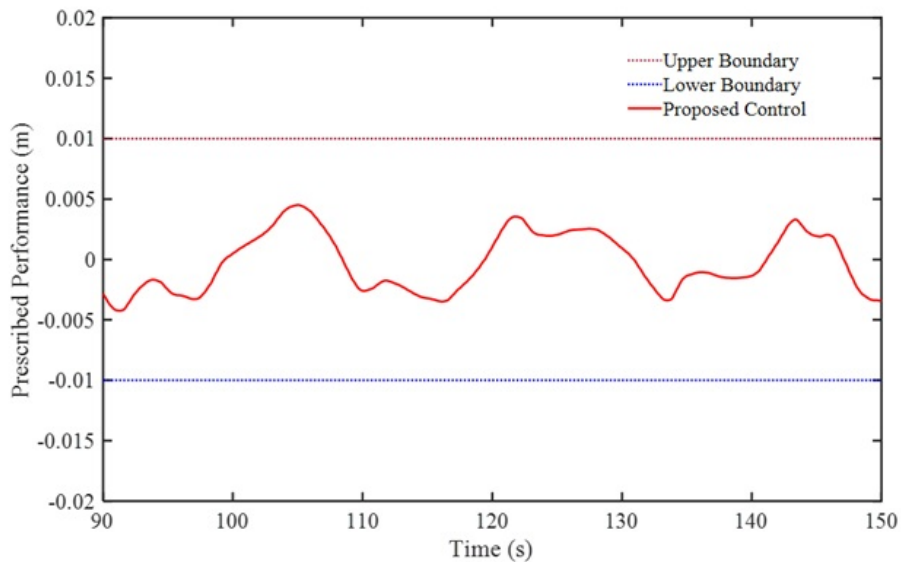
Figure 9: Prescribed performance of the proposed control for displacement of seat system: (a) general view, (b) large view.
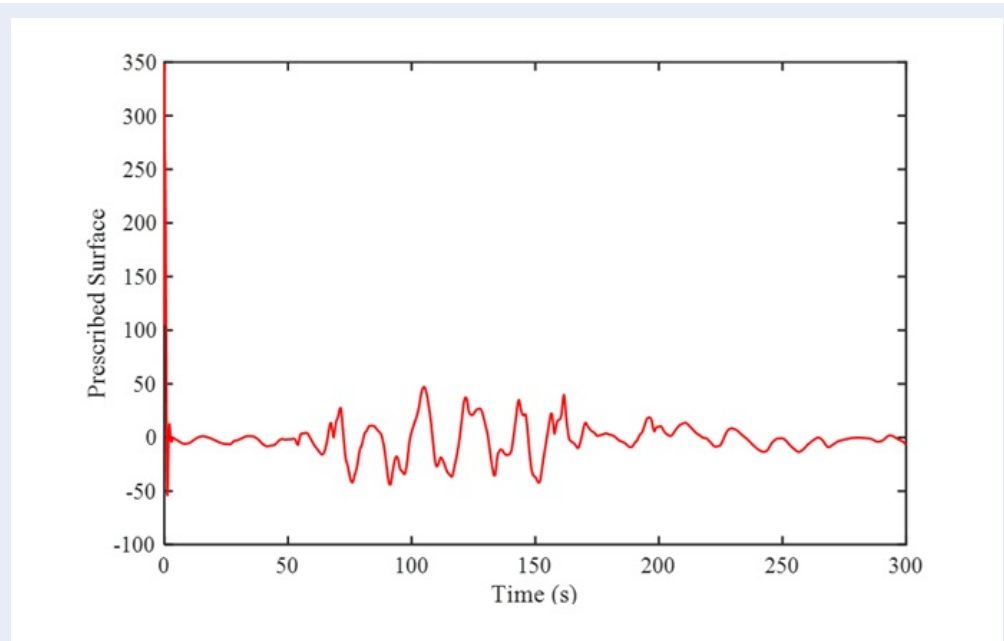
Figure 10: Prescribed surface of the proposed control.
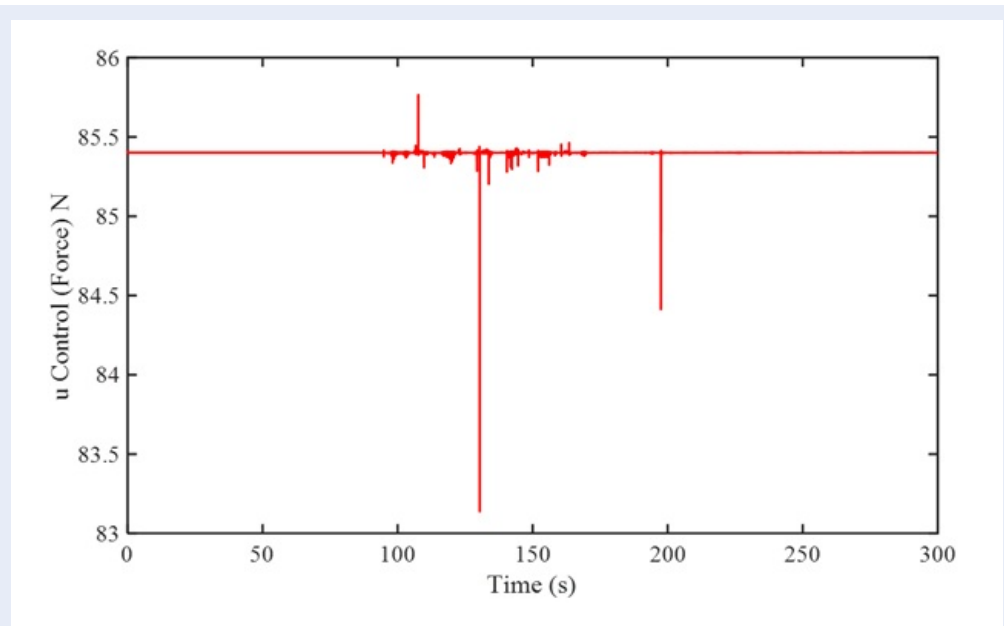
Figure 11: Damping force control for the seat model with the proposed controller.
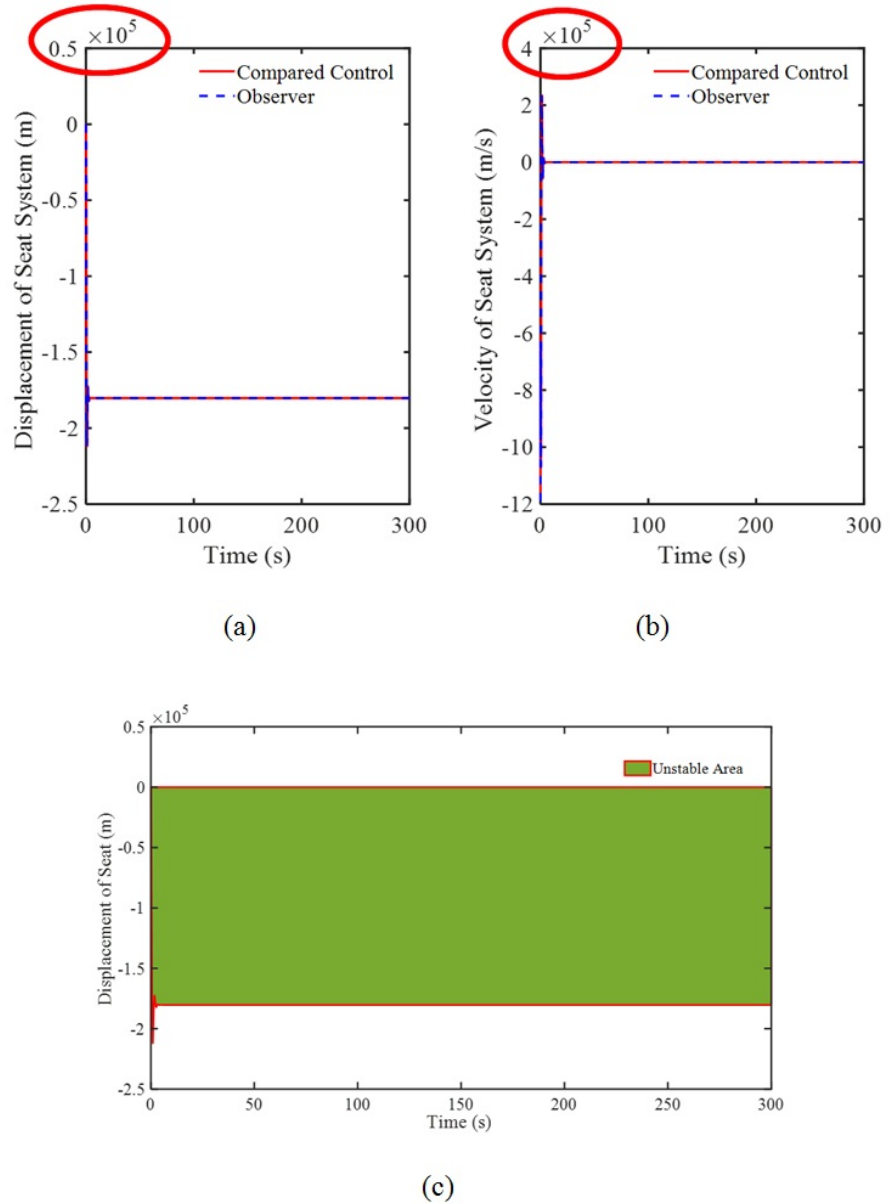
Figure 12: Displacement of seat system of the compared control: (a) Displacement, (b) Velocity, (c) Unstable area view of displacement.

is shown that the controlled force is always lower than the setup value 1000 N. This proves that the proposed control is to save the consumption of energy. Results of the compared control are shown in Figures 12, 13 and 14. In Figure 12, the performance of the seat system is not good and the output value is always in the unstable area as shown in Figure 12c. As mentioned above, the performance of the driver is following the seat vibration. Hence, the driver response is also not good as shown in Figure 13. Furthermore, the con-

trol energy following the damping force of the compared control also obtains the maximal value 1000 N as shown in Figure 14. This point shows that the compared control uses the maximal value of input control and the obtained results are not good. To conclude the proposed control and the compared control based on the variation of power for control and the frequency, the power spectral density (PSD) graph as shown in Figure 15 shows that the proposed control always guarantees the stability of the system which is
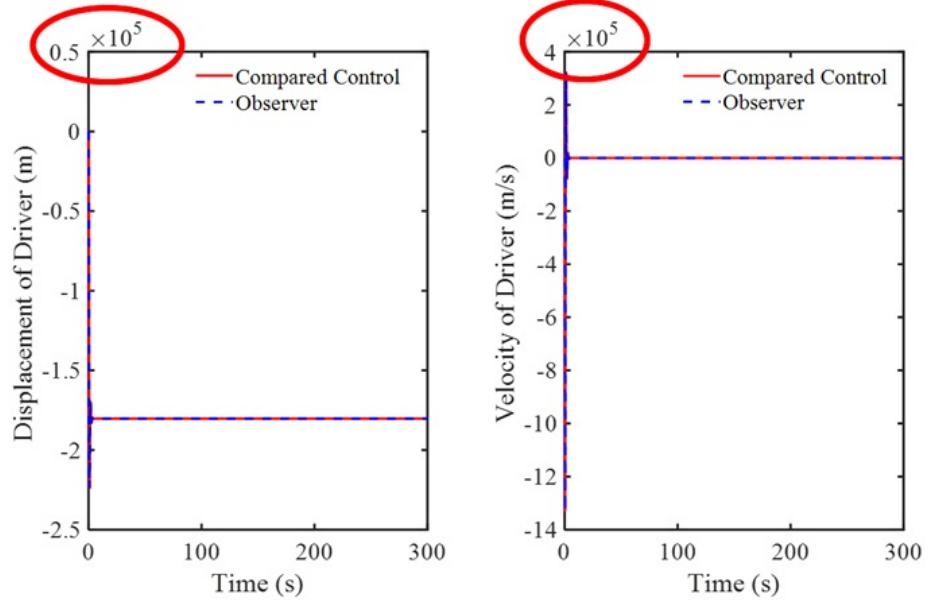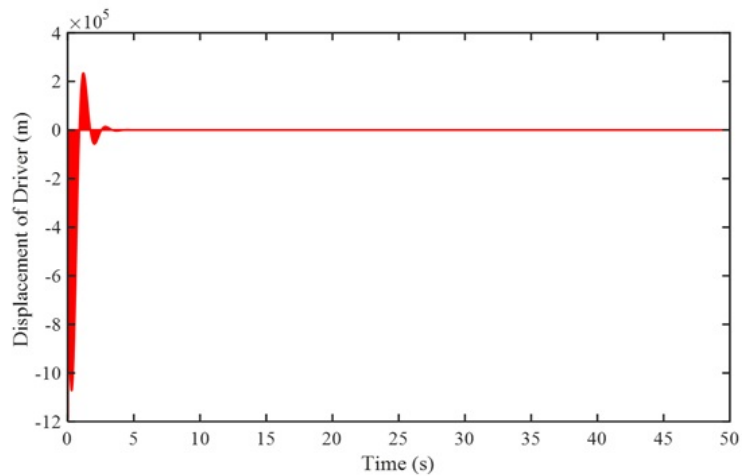
Figure 13: Displacement of driver of the compared control: (a) Displacement, (b) Velocity, (c) Unstable area view of displacement.

better than the compared control. Figure 15 is also show that the proposed control can save the energy of control better than the compared control.

CONCLUSIONS

A new robustness controller was proposed and applied in this study for vibration control of a vehicle seat system. The controller includes two sliding surfaces as conventional and prescribed model. From the proposed surfaces, the main input controller was designed with its constraints related Lyapunov function. The stability of the controller was proved based on Lyapunov candidate and LMI method. After analyzing, the controller is is simulated and compared with an existing controller[19]. The compared results show that the proposed controller obtains good performance under severe disturbances in both stability and saving energy. In future work, the technique of
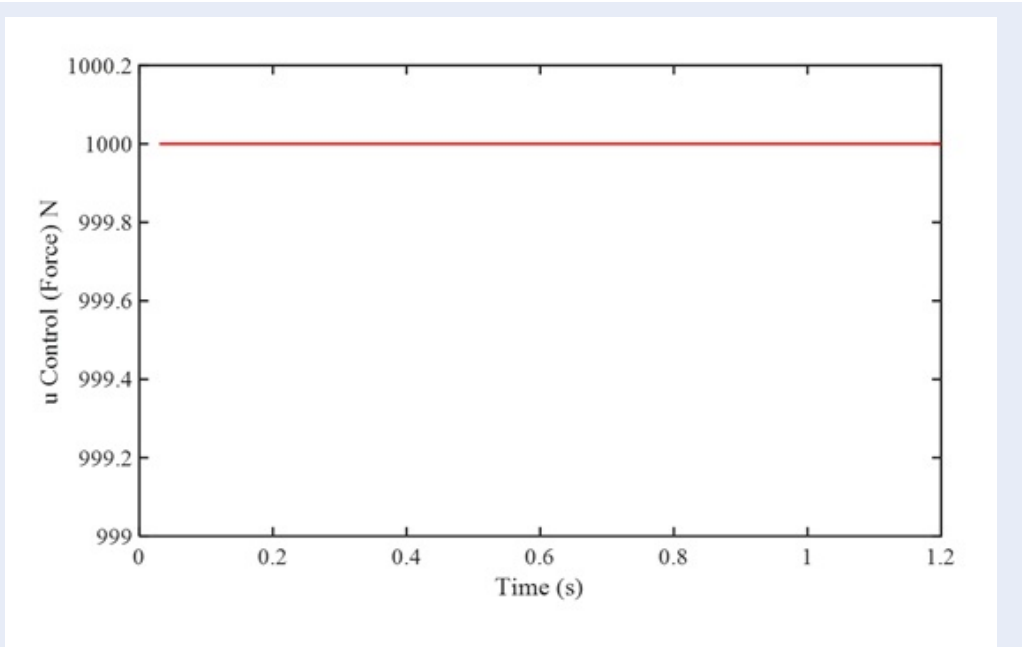
Figure 14: Damping force control for the seat system with the compared control.
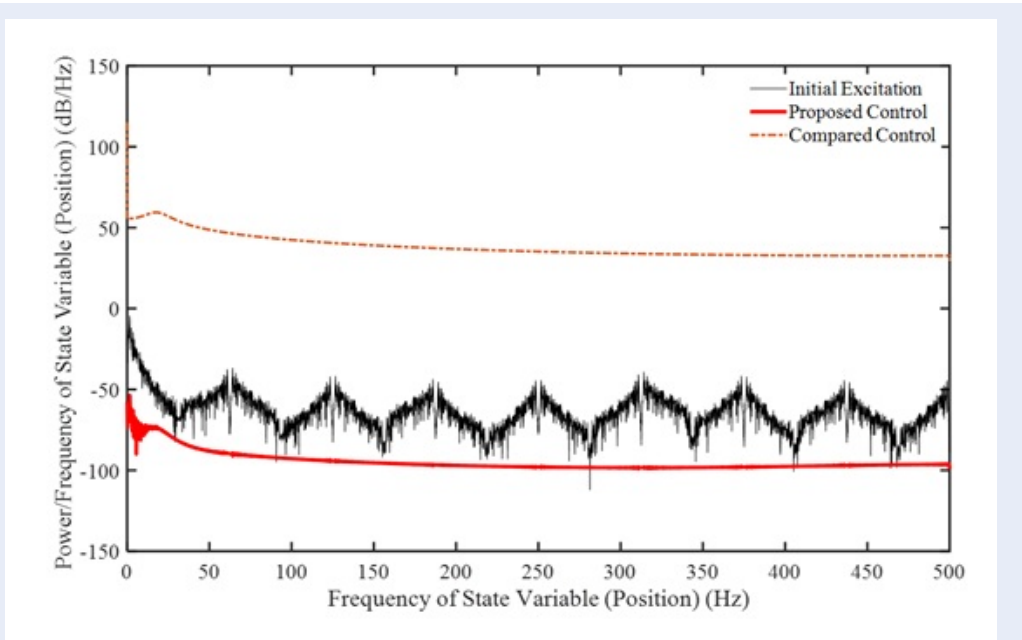
Figure 15: PSD of random step wave road for the proposed controller and the compared controller[19].

this research will concentrate on analyzing the affection of a switching controller to a real model, to improve its flexibility in complicated models.

ACKNOWLEDGEMENT

DECLARATION OF CONFLICTING INTEREST

The authors declare that there is no conflict of interest.

AUTHORS' CONTRIBUTION

Do Xuan Phu: conceptualization, methodology, software, writing-original draft preparation.

Nguyen Quoc Hung: Data curation, writing, reviewing and editing.

REFERENCES

1. Sun W, Wu YQ, Sun ZY. Command filter-based finite-time adaptive fuzzy control for uncertain nonlinear systems with prescribed performance, IEEE Transactions on Fuzzy Systems. 2020;Available from: https://doi.org/10.1109/TFUZZ.2020.2967295.
2. Shi W. Adaptive fuzzy output feedback control for non-affine MIMO nonlinear systems with prescribed performance, IEEE Transactions on Fuzzy Systems. 2020;Available from: https://doi.org/10.1109/TFUZZ.2020.2969110.
3. Van M, Ge SS. Adaptive fuzzy integral sliding mode control for robust fault tolerant control of robot manipulators with disturbance observer, IEEE Transactions on Fuzzy Systems. 2020;Available from: https://doi.org/10.1109/TFUZZ.2020.2973955.
4. Sun W, Lin JW, Su SF, Wang N, Er MJ. Reduced adaptive fuzzy decoupling control for lower limb exoskeleton, IEEE Transactions on Cybernetics. 2020;Available from: https://doi.org/10.1109/TCYB.2020.2972582.
5. Yu W, Rosen J. Neural PID control of robot manipulators with application to an upper limb exoskeleton, IEEE Transactions on Cybernetics. 2013;43(2):673–684. Available from: https://doi.org/10.1109/TSMCB.2012.2214381.
6. Sangpet T, Kuntanapreeda S, Schmidt R. An adaptive PID-like controller for vibration suppression of piezo-actuated flexible beams, Journal of Vibration and Control . 2018;24(12):2656–2670. Available from: https://doi.org/10.1177/1077546317692160.
7. Van M, Do XP, Mavrovouniotis M. Self-tuning fuzzy PID-nonsingular fast terminal sliding mode control for robust fault tolerant control of robot manipulators ISA Transactions. 2020;96:60–68. Available from: https://doi.org/10.1016/j.isatra.2019.06.017.
8. Phu DX, An JH, Choi SB. A novel adaptive PID controller with application to vibration control of a semi-active vehicle seat suspension, Applied Sciences. 2017;7(10):1055. Available from: https://doi.org/10.3390/app7101055.
9. Phu DX, Huy TD, Mien V, Choi SB. A new composite adaptive controller featuring the neural network and prescribed sliding surface with application to vibration control, Mechanical Systems and Signal Processing. 2018;107:409–428. Available from: https://doi.org/10.1016/j.ymssp.2018.01.040.
10. Do XP, Nguyen QH, Choi SB. New hybrid optimal controller applied to a vibration control system subjected to severe disturbances, Mechanical Systems and Signal Processing. 2019;124:408–423. Available from: https://doi.org/10.1016/j.ymssp.2019.01.036.
11. Phu DX, Choi SM, Choi SB. A new adaptive hybrid controller for vibration control of a vehicle seat suspension featuring MR damper, Journal of Vibration and Control . 2017;23(20):3392–3413. Available from: https://doi.org/10.1177/1077546316629597.
12. Guo XG, Ahn CK. Adaptive fault-tolerant pseudo-PID sliding-mode control for high-speed train with integral quadratic constraints and actuator saturation, IEEE Transactions on Intelligent Transportation Systems. 2020;Available from: https://doi.org/10.1109/TITS.2020.3002550.
13. Martınez-Fuentes CA, Seeber R, Fridman L, Moreno JA. Saturated Lipschitz continuous sliding mode controller for perturbed systems with uncertain control coefficient, IEEE Transactions on Automatic Control. 2020;Available from: 0.1109/TAC.2020.3034872.
14. Fallaha C, Saad M, Ghommam J, Kali Y. Sliding mode control with model-based switching functions applied on a 7-dof exoskeleton arm, IEEE/ASME Transactions on Mechatronics. 2021;26(1):539–550. Available from: https://doi.org/10.1109/TMECH.2020.3040371.
15. Long Y, Peng Y. Extended state observer-based nonlinear terminal sliding mode control with feedforward compensation for lower extremity exoskeleton, IEEE Access. 2021;Available from: https://doi.org/10.1109/ACCESS.2021.3049879.
16. Zhang X. Robust integral sliding mode control strategy under designed switching rules for uncertain switched linear systems via multiple Lyapunov functions, Transactions of the Institute of Measurement and Control. 2019;41(12):3536–3549. Available from: https://doi.org/10.1177/0142331219832947.
17. Wang H, Fang L, Hu M, Song T, Xu J. Adaptive funnel fast nonsingular terminal sliding mode control for robotic manipulators with dynamic uncertainties, Proc IMechE Part C: J Mechanical Engineering Science. 2020;Available from: https://doi.org/10.1177/0954406220978269.
18. Nechak L. Robust Nonlinear Control of Mode-Coupling-Based Vibrations by Using High-Gain Observer and Sliding-Mode Controller, Journal of Dynamic Systems, Measurement, and Control. 2021;143. Available from: https://doi.org/10.1115/1.4048356.
19. Zimenko K, Polyakov A, Efimov D, Perruquetti W. Robust feedback stabilization of linear MIMO systems using generalized homogenization, IEEE Transactions on Automatic Control. 2020;Available from: https://doi.org/10.1109/TAC.2020.2969718.
20. Ciccarella G, et al. A Luenberger-like observer for nonlinear systems, International Journal of Control. 1993;57(3):537–556. Available from: https://doi.org/10.1080/00207179308934406.

Open Access Full Text Article

Điều khiển cho các hệ thống phi tuyến dựa trên hệ điều khiển trượt với biên dạng đồng nhất xác định

Đỗ Xuân Phú[1,*], Nguyễn Quốc Hưng[2]

TÓM TẮT

Bài báo giới thiệu một thuật toán điều khiển mới dựa trên mô hình điều khiển trượt kép và điều khiển tăng cường dùng các ràng buột theo phương pháp ma trận bất tuyến tính (LMI). Điều khiển đề nghị được áp dụng cho hệ thống bị nhiễu nặng. Hàm mặt trượt trong điều khiển trượt gồm hai phần: phần hàm mũ và hàm liên quan định thức kiểu t (t-norm) để tiết kiệm năng lượng trong quá trình điều khiển hệ thống. Các phương trình ràng buột liên quan LMI được đề nghị gồm các ma trận và vec-tơ theo phương pháp chọn để đảm bảo nguồn năng lượng cho điều khiển. Việc giải các ràng buột cũng được giới thiệu trong bài báo theo hướng tiết kiệm thời gian tính toán. Thêm vào đó, việc chứng minh thuật toán điều khiển cũng được giới thiệu với các phương trình Lyapunov. Trong hàm điều khiển đầu vào, dạng định thức t được dùng để cải thiện khả năng điều khiển nhiễu. Ngoài ra dạng định thức t, dạng mặt trượt biến đổi trong hàm điều khiển đều vào cũng được cải tiến với mục tiêu tiết kiệm năng lượng. Sự kết hợp của các thành phần này mang đến khả năng mới cho thiết kế điều khiển. Sự vượt trội của điều khiển đề nghị được minh chứng qua mô phỏng với hệ thống giảm sốc ở ghế ngồi xe. Hệ thống giảm sốc dùng một giảm chấn lưu chất từ biến và dạng nhiễu ngẫu nhiên được dùng trong mô phỏng này. Một thuật toán so sánh từ nghiên cứu hiện tại được dùng để đánh giá kết quả của thuật toán đề nghị. Thuật toán so sánh có cấu trúc khá giống với thuật toán đề nghị. Các kết quả mô phỏng cho thấy thuật toán đề nghị mang đến khả năng tốt hơn và ổn định hơn cho hệ thống. Tính ổn định của thuật toán được đánh giá qua năng lượng đầu vào và biểu đồ năng lượng phổ (PSD) liên quan năng lượng tiêu thụ.

Từ khoá: điều khiển đồng nhất, điều khiển trượt, mặt trượt, điều khiển dao động, hệ thống giảm sốc ghế

[1]*Khoa Cơ Điện tử và công nghệ cảm biến, trường Đại học Việt Đức, Bình Dương, Việt Nam*

[2]*Khoa Kỹ thuật tính toán, trường Đại học Việt Đức, Bình Dương, Việt Nam*

Liên hệ

Đỗ Xuân Phú, Khoa Cơ Điện tử và công nghệ cảm biến, trường Đại học Việt Đức, Bình Dương, Việt Nam

Email: phu.dx@vgu.edu.vn

Check for updates

VNU-HCM Press